10-24-2022

River Discharge Mediates Extent of Phytoplankton and Harmful Algal Bloom Habitat in the Columbia River Estuary (USA) During North Pacific Marine Heat Waves

Taylor N. Dodrill
Portland State University, tdodrill@pdx.edu

Yangdong Pan
Portland State University, pany@pdx.edu

Tawnya D. Peterson
Oregon Health and Science University

Citation Details

Published as: Dodrill, T. N., Pan, Y., & Peterson, T. D. (2022). River Discharge Mediates Extent of Phytoplankton and Harmful Algal Bloom Habitat in the Columbia River Estuary (USA) During North Pacific Marine Heat Waves. Estuaries and Coasts, 1-16.

River Discharge Mediates Extent of Phytoplankton and Harmful Algal Bloom Habitat in the Columbia River Estuary (USA) During North Pacific Marine Heat Waves

Taylor N. Dodrill[1], Yangdong Pan[1], Tawnya D. Peterson[2]

[1]Dept. of Environmental Science and Management, Portland State University, Portland, OR 97201, USA

[2]School of Public Health, Oregon Health & Science University, Portland, OR 97239, USA

The e-mail address, telephone and fax numbers of the corresponding author: tdodrill@pdx.edu, (541) 868-5490.

Acknowledgements

We would like to thank L. Cook for his assistance with field collections and light microscopic identification, and S. Dyer and A. Bryn for their help with field work. In addition, we would like to thank the captain and crew of the R/V *Oceanus* for assistance in sample collection. This work was funded by a National Science Foundation Graduate Research Fellowship to TND, the Lower Columbia River Estuary Partnership's Ecosystem Monitoring Program, and the Center for Coastal Margin Observation and Prediction (CMOP; NSF-OCE 0424602). We also thank CMOP, the United States Geological Survey (USGS), and Columbia River Data Access in Real Time (DART) for the use of publicly available data.

Abstract

Marine heat waves (MHW) have been associated with extensive harmful algal blooms (HABs) in the northeast Pacific Ocean, but the degree to which these large-scale oceanographic events are mirrored in nearshore environments has not been well established. We compared phytoplankton assemblages in the Lower Columbia River Estuary (LCRE) during two Pacific MHWs that took place in 2015 and 2019, with observations from 2017, a year with no MHW. These data were paired with environmental data from the summers of 2015 - 2019 to characterize differences in estuarine conditions during MHWs that promote phytoplankton assemblage transitions, and identify HAB-conducive conditions. Bloom densities of HAB taxa, *Pseudo-nitzschia* spp. (4.16×10^6 cells L^{-1}) and *Gymnodinium catenatum* (5.66×10^6 cells L^{-1}), were noted in the estuary during 2015 and 2019, respectively, two years where Pacific MHWs occurred during the summer months. These blooms coincided with estuary temperatures that were 1-2 ℃ above and river discharge volumes 46-48% lower than decadal daily averages. We identified patterns in the densities of several algal taxa associated with MHW-mediated low discharge in the LCRE, such as declines in tychopelagic diatoms and increasing abundance of pelagic marine taxa. We conclude that low river discharge, through extension of saline habitat area and longer residence times, likely contributed to the development of the observed marine HABs in the estuary. MHWs and associated declines in discharge are projected to become more common in the Pacific Northwest with climate change, which may alter late summer phytoplankton assemblages in the LCRE.

Key words: Harmful algal blooms, marine heat waves, estuarine ecology, discharge, *Gymnodinium catenatum, Pseudo-nitzschia*

Introduction

Harmful algal blooms (HABs) are occurring more frequently on a global scale, a phenomenon connected to climate change (Hallegraeff 1993, 2010; Van Dolah 2000; Lewitus et al. 2012). HABs often result in fishery closures due to the production of algal toxins, which can accumulate in consumers. Closures aid in protecting public health, but can destabilize commercial and recreational fisheries, create declines in fisheries and tourism revenue, and impact residents' food security, cultural activities, and quality of life (Dyson and Huppert 2010; Poe et al. 2015; Berdalet et al. 2016; Ritzman et al. 2018). The northeast Pacific Ocean experienced a long-lived, persistent MHW, commonly called "The Blob", that began in the winter of 2013, peaked in 2014-2015, and dissipated in 2016 (Bond et al. 2015; Di Lorenzo and Mantua 2016). A shorter-lived MHW (given the name "Blob 2.0") appeared during the summer of 2019 and disappeared after approximately four months (Amaya et al. 2020). Negative ecosystem effects, including a massive marine HAB, associated with The Blob have been extensively documented in the northeast Pacific Ocean (Du et al. 2016; McCabe et al. 2016; Brodeur et al. 2019; Rogers-Bennett and Catton 2019; von Biela et al. 2019; Piatt et al. 2020). Previous temperature anomalies in the Northeast Pacific coastal ocean have resulted in impacts to phytoplankton biomass, productivity, and community composition (Kudela et al. 2006). MHWs can also alter estuarine ecosystems, but HAB studies along the U.S. West Coast have focused on offshore and coastal habitats, leaving gaps in our knowledge of how atmospheric phenomena impact estuaries. Several studies on estuaries outside the Pacific Northwest suggest heat waves negatively affect estuarine water quality (e.g., increased biological oxygen demand, cyanobacteria blooms, low DO, low pH, and microbial pathogen growth) (Wetz and Yoskowitz 2013; Tassone et al. 2022). To our knowledge there is only one published observation of a localized heat wave linked to a

HAB within a U.S. west coast estuary (Cloern et al. 2005). Other than this event, the 2015 and 2019 events are the only recorded MHWs associated with estuarine HABs for the region. Though MHW-associated HABs have been observed globally (Roberts et al. 2019; Gao et al. 2021), this field of study is relatively young and events where these phenomena are linked are somewhat sparse (Hobday et al. 2018). Other HABs have been documented in Pacific Northwest estuaries, but were not linked to heat waves and were associated with transport from coastal waters (Lewitus et al. 2012). In the LCRE, algal blooms are relatively rare, with the exception of a recurring late summer *Mesodinium rubrum* bloom (Herfort et al. 2011). In this study, we refer to phytoplankton cell concentrations on the order of 10^4 cells L^{-1} or greater as a bloom. We set this quantitative definition because both *Pseudo-nitzschia australis* and *Gymnodinium catenatum* are known to produce levels of domoic acid and saxitoxins, respectively, that result in consumer contamination at this density (Lefebvre et al. 2002; Costa et al. 2010). This threshold identifies algal densities impactful for fisheries management due to toxin contamination of harvested species.

The LCRE, like the majority of large Pacific Northwest estuaries, is freshwater-dominated (Heady et al. 2014), and therefore thought to be less impacted by oceanographic events like MHWs. Columbia River hydrology is largely influenced by snowpack in low-elevation mountain ranges, with plentiful winter precipitation that falls as rain or snow depending on temperatures, a spring freshet, and dry summers (Tohver et al. 2014). Atmospheric influences such as the position of the deep Aleutian low of the Pacific/North American circulation pattern, El Nino/Southern Oscillation (ENSO) and disruptions of the jet stream, which can contribute to the formation of MHWs, have a large influence on snowpack, and the resulting timing and volume of snowmelt runoff to the LCRE (Cayan 1996; Clark et al. 2001;

Mote 2006). The flow regime of the Columbia River is also influenced by a series of storage and run-of-the-river dams (Federal Columbia River Power System 2001). Flow rates to the LCRE may be altered during drought years due to lower snowpack [e.g. 2014-2015 Pacific Northwest "snowpack drought" (Boniface et al. 2016)], warmer temperatures, and exceptionally low summer flows; all characteristics projected under climate change for the region (Hamlet and Lettenmaier 1999). Although the LCRE is river-dominated for much of the year, oceanographic conditions develop during the summer months when river flow is at its lowest (Chawla et al., 2008), creating an inverse relationship between discharge and salinity. Oceanographic inputs to the estuary affect water quality, for example, delivery of upwelling-derived nitrate through tidal exchange (Bruland et al. 2008). The shifts from freshwater-dominated to brackish-marine conditions is reflected in the seasonal succession of estuarine plankton (Rollwagen-Bollens et al. 2020). Therefore, the vulnerability of the LCRE to the ecological effects of MHWs could differ significantly depending on the timing of their occurrence.

In this study, we compare phytoplankton assemblages of the LCRE during two MHWs (2015 and 2019) that differed in extent and timing with those in 2017 without MHW. Our study objectives are to (1) characterize differences in estuarine conditions during MHWs that may promote HABs, and (2) identify phytoplankton assemblage characteristics to aid in identifying transitions to HAB-conducive conditions. This work provides insight into the LCRE's algal community response to two MHWs of differing persistence, and evaluates how hydrologic forcing could play an important role in mediating the impact of MHWs in the LCRE. Particularly during anomalous oceanographic events, understanding the degree and timing of ocean-estuary connectivity is crucial to predicting algal community shifts in estuarine habitat.

Methods

Study area

The LCRE is a river-dominated, drowned river mouth estuary (Heady et al. 2014), with the fourth largest river volume in the United States (Baptista et al. 2015) (Fig. 1). The LCRE food web is largely detritus-driven, and phytoplankton grazing makes up the main living component of food resources for primary consumers (Simenstad et al. 1990). Haertel and Osterberg (1967) described three main groups of plankton in the LCRE: those associated with freshwater, marine plankton that are transported into the estuary from the coast, and plankton indigenous to the estuary that are associated with brackish waters. The study took place at a site in Ilwaco Harbor in Baker Bay, a shallow (<15 m depth) bay just upstream of the river mouth (~5 km) on the northern side of the estuary. We also sampled two nearby sites in the mainstem of the LCRE on the southern side of the estuary during a research cruise aboard the R/V *Oceanus* (Fig. 1a).

Sample collection and analyses

The majority of phytoplankton samples (total n = 24) were collected from the surface at Ilwaco Harbor (n=18), with additional samples collected in September-October 2015 (n=6) aboard the R/V *Oceanus,* which provided data on the depth distribution of phytoplankton in the LCRE (surface, mid-depth, and bottom). Surface samples at the Ilwaco site in 2015 and 2017 were collected approximately monthly during the spring and summer of these years, while samples were collected monthly June - July of 2019 and fortnightly August - October of 2019 (Fig. 1b). Whole water samples were collected for algal identification and enumeration using clean glass French square bottles. Samples were preserved in Lugol's Iodine solution (final concentration, 1%). Samples were homogenized and settled in an Utermöhl sedimentation chamber for 24 h and cells were identified and enumerated using a Leica DMIL inverted microscope. Cells were enumerated up to 400 counting units, using 100X, 200X, and 400X magnification, each for several of fields of view per sample in order to adequately capture both smaller cells and rarer, larger taxa. Where replicate samples were available, counts were averaged. Where possible, cells were identified to genus or species, and in some cases complexes or groups that were more practical for identification using light microscopy. For example, species within the genus, *Pseudo-nitzschia*, cannot be identified to species with a light microscope alone; individuals were therefore classified into complexes of *Pseudo-nitzschia* c.f. *australis/fraudulenta*, *P.* c.f. *pungens/multiseries,* or *P.* c.f. *pseudodelicatissima/delicatissima*, which can be differentiated by cell size and shape (e.g., length: width ratio) (Trainer and Suddleson 2005). Phytoplankton abundances are reported as cell concentrations or as a proportion of the total cells counted in the sample. Simpson's Diversity Index (D) was calculated using the '*vegan*' package in R (Simpson 1949).

Collection and analysis of environmental data

Environmental data were collected using continuous sensors at the SATURN-03 endurance station (Fig. 1; www.stccmop.org), including salinity (every 15 s), temperature (every 15 s), chlorophyll (every 3 min), and nitrate (every hour) at three depths (2.4 m, 8 m, and 13 m). Chlorophyll fluorescence was measured using an *in situ* fluorometer (Turner Designs AlgaeWatch in 2015 and a Turner Designs Cyclops in 2019) and calibrated against extracted chlorophyll a (S. Riseman, pers. comm.), and nitrate was measured using an *in situ* ultraviolet spectrophotometer (ISUS Satlantic in 2015, SUNA Seabird Scientific in 2019). Although the SATURN-03 sensor is located across the channel from the water sampling site, we determined that data collected from this sensor suite (i.e., salinity, temperature, nitrate) were highly similar to measurements from grab samples collected at Ilwaco Harbor (data not shown). Discharge data were downloaded from the USGS river gauge at Quincy Washington/Beaver Army Terminal at river mile 53 (river km 85), a point downstream from major tributaries (USGS 2022). Upwelling index data were obtained from the DART Pacific Ocean Coastal Upwelling Index Dataset, courtesy of the National Marine Fisheries Service, Pacific Fisheries Environmental Laboratory (Columbia River DART, Columbia Basin Research, and University of Washington 2021). Upwelling index values were derived from estimated Ekman transport based on mean surface atmospheric pressure fields for every 6 h at the Lincoln City, OR standard location. This index summarizes the direction and velocity of water movement, with positive values representing offshore water movement (upwelling), and negative values representing onshore movement (downwelling). Data for each environmental variable were initially averaged hourly, and were used to calculate day equivalents of elevated temperature and salinity conditions by adding all hours above a certain threshold together and dividing by 24 h (Tables 1, 2). To limit noise from diurnal tidal action, all data for each environmental variable were averaged daily for the generalized additive mixed model analysis. Sensor data were smoothed by calculating 14-d rolling daily averages to capture conditions in the window leading up to each phytoplankton sampling event prior to use in the gradient forest analysis.

Algal toxin analysis

A whole water sample for toxin analysis was collected concurrently with each algal sampling event, filtered onto GF/F filters (400 – 1000 mL per sample, depending on algal density), and frozen at -20ºC, pending analysis. Samples in which toxic algal species were present, as determined using light microscopy, were prioritized for toxin analysis of seston (total: *n*=10, October 2015: *n*=6, August-October 2019: *n*=4). Analytes were extracted from filters in deionized water with sonication as in Lefebvre et al. (2008), and four analytical replicates per sample were analyzed. We used ELISA kits (Mercury Science Inc.) and a Molecular Devices Spectra Max M2^e plate reader with the necessary toxin standards and controls to assess concentrations of domoic acid (typically reported in ng L^{-1}) and total saxitoxins (typically reported in ppb), the toxins produced by *Pseudo-nitzschia* spp. and *G. catenatum*, respectively. We did not collect shellfish samples during the study to understand whether the algal toxin production translated to accumulation of toxins in shellfish tissues.

Statistical analyses

We used generalized additive mixed models (GAMMs) to characterize the environmental conditions during May through October of 2015 - 2019, the season when HABs most commonly occur, while reducing the variation of environmental variables due to well-documented seasonal changes (Rollwagen-Bollens et al. 2020). We identified periods of statistically significant environmental change in a time series of daily averages of multiple water quality variables using the '*mgcv*' package in R, with Gaussian probability distributions of the variables, and the restricted maximum likelihood (REML) method for smoothness selection (Wood 2017, Simpson 2018). Temporal autocorrelation was explicitly modeled in the GAMM, and model selection was determined by comparing Bayesian Information Criterion (BIC) of models with different error correlation structure and checking for autocorrelation among model residuals.

We used a non-metric multidimensional scaling (NMDS) analysis with the Bray-Curtis dissimilarity index to assess patterns in species composition (Clarke 1993). Species count data were square-root-transformed prior to the NMDS, which was done using the R package '*vegan*' (Oksanen et al. 2011). Vectors of environmental variables were fitted to the NMDS plot using the envfit function in the same package. We used agglomerative hierarchical clustering with average linkage on a Bray-Curtis dissimilarity matrix to find grouping patterns in the phytoplankton assemblage dataset.

We used gradient forest analysis to identify thresholds separating components of phytoplankton assemblages along major environmental gradients. This analysis was performed using the '*extendedForest*' and '*gradientForest*' packages in R (v3.6.2; Ellis et al. 2012). A gradient forest fits a random forest model for each taxon in the phytoplankton assemblage, in which each of 500 trees is fit to a bootstrapped sample and splits are made using a random subset of predictors. Goodness-of-fit R^2 values for each taxon can be distributed in proportion to the importance of each predictor to generate the overall importance of a predictor to phytoplankton species composition. Split density plots show where (on the scale of the predictor) a predictor is splitting trees, and indicate the importance of each predictor based on how much of the variance in the data it explains. Compositional turnover plots show cumulative importance of predictors for each species over gradients of predictor variables. Taxa present in <5% of samples or at very low cell concentrations (< 10 cells ml^{-1}) were excluded from the gradient forest analysis.

Results

Estuarine conditions

Daily average surface water temperatures in the LCRE were elevated by ~1-2 ºC in July-December of 2015 and July-September of 2019, relative to the decadal average at the SATURN-03 site (Fig. 2). For summers included in the study period, temperatures typically increased most rapidly through May and June, peaked in the window of July-September, and began to decrease in September or October (Fig. 2).

Elevated surface temperatures were sustained for a longer period of time during 2015 and 2019 than for any other year during the study period (approximately 49.0 and 47.4 day equivalents >18 °C; 18.3 and 12.8 day equivalents >20 °C, respectively) (Table 2). In addition, temperatures did not drop as rapidly during the summer-autumn transition in 2015 as was observed during 2016-2019 (Fig. 3).

Hydrographs for the LCRE varied greatly among the five years. In 2017, a non-MHW year with a strong spring freshet and high discharge throughout the growing season, peak discharge was 111% higher and minimum discharge was 4% lower than the decadal average (Fig. 2). Discharge in 2018 and 2019 also displayed a large freshet pattern, with peak daily average discharges 83% and 92% higher than the decadal average, respectively. The spring freshet was smaller in 2015 and 2016; peak flows were 53% and 5% higher than the decadal average, respectively. For all study years but 2017, minimum discharge was 42 - 76% lower than the decadal average minimum (Fig. S1).

Salinity in the LCRE increased throughout May - October each year, with daily averages <5 PSU typical in May, and >10 PSU typical of late summer. In 2015, however, the smoothed daily average salinity in June was >10 PSU (Fig. 3). The summer of 2015 also had the highest number of day equivalents (7.1 d) of salinity >25 PSU at 2.4 m, compared to a range of 3.8 - 4.4 d for the other years studied (Table 1), showing an extended period of strong marine influence on the surface waters of the LCRE. We observed an extended period of brackish surface water in 2019, which had 72.5 day equivalents of salinity >15 PSU at 2.4 m, compared to a range of 45.5 - 60 d in 2015 – 2018 (Table 1).

Upwelling patterns were similar among years, with the exception of a significant shift toward downwelling in late summer of 2016 (> 0 $m^3 s^{-1} 100 m^{-1}$), and an earlier peak in upwelling (~120 $m^3 s^{-1} 100 m^{-1}$ in June) and a significant decline in the rate of offshore transport throughout the summer of 2019 (Fig. 3). The highest nitrate concentrations (>20 µM in May 2016-2018) were observed in early summer, with some fortnightly fluctuations. Nitrate concentrations were lower on average in 2015 than other study years, especially earlier in the season (<10 µM in May). No nitrate data were collected in 2019 (Fig. 3). Chlorophyll showed fortnightly variation, with higher overall chlorophyll levels earlier in the summer that decreased as the summer progressed. We observed a small peak in chlorophyll during the 2015 bloom of *Pseudo-nitzschia* spp. and the 2019 *G. catenatum* bloom (z-scores of 1.8 and 2.8, respectively) (Fig. 3).

Algal species composition

We identified 168 species or species complexes and 112 genera, with a mean richness of 25 taxa per sampling date and average sample diversity D of 0.70 (range = 0.17 to 0.91) over the three years for which phytoplankton samples were collected. We identified six phyla (Bacillariophyta, Chlorophyta, Cryptophyta, Cyanophyta, Dinoflagellata, Euglenophyta) and two taxonomically amalgamated groups to capture other less common taxa (small flagellates, and other). Bacillariophyta typically dominated the assemblages, with an average relative abundance of 56%. Among phylum Bacillariophyta, *Navicula* spp. were abundant on all sampling dates, peaking at 69% of total cells in April 2017. *Melosira varians, Skeletonema* spp., and c.f. *Cyclotella/Thalassiosira* spp. were the next most abundant diatoms in spring/early summer. Dinoflagellata had an average relative abundance of 29%, and each of the other taxonomic groups had an average relative abundance of <10% (Fig. 2). A NMDS analysis (stress = 0.12) indicated that phytoplankton samples varied most along the first NMDS axis (Fig. 4) with greater separation of samples among years (i.e., 2015 and 2019 vs. 2017) and seasons (i.e., late summer vs. early summer samples from 2015 and 2019).

Hierarchical cluster analysis indicated that the two algal blooms observed in the study were distinctly different in composition. In 2015, the toxigenic marine diatoms, *Pseudo-nitzschia* spp. (mostly from the *P.* c.f. *australis/fraudulenta* group), dominated the phytoplankton assemblage in early October (average of 56% on 10/1/2015; Fig. 2), in contrast to other sampling dates, which had either undetectable or low (March 2017, August-September 2019) *Pseudo-nitzschia* spp. concentrations. Particulate domoic acid (pDA) was measured at relatively low, but detectable, levels during the *Pseudo-nitzschia* spp. bloom (Fig. 6). Average toxin concentrations ranged from 41－86 ng L^{-1} from samples taken at the bottom (~13 m), middle (~8 m) and surface of the water column on October 1 and mid water column on October 2, 2015. Although domoic acid was detected at ~8 m, it was not detected at the bottom or surface on October 2. In 2019, the chain-forming marine dinoflagellate, *Gymnodinium catenatum*, peaked at 91% of the total assemblage in mid-August; the bloom persisted through late September. It was not detected in our light microscopy analyses any time outside this bloom period. Once the bloom began to decline (*ca.* 9/12/2019), *G. catenatum* was accompanied by *Euglena* sp. (24%), *Cryptomonas erosa* (16%), and *Mesodinium rubrum* (5%). Overall, species diversity during the peak of the 2019 bloom was very low (D = 0.17) compared to the highest reported diversity from earlier that year (D = 0.80 on 7/10/2019). Saxitoxins were detected during the *G. catenatum* bloom, ranging from 1.14－1.79 ppb, with the highest toxin level detected during the height of the bloom in late August (Fig. 6).

Environmental drivers of phytoplankton assemblage composition

Ordinations with overlaid environmental vectors with points scaled by the relative abundance of phytoplankton taxa (Fig. 5) indicated that densities of the marine planktonic diatoms like *Ditylum brightwellii, Thalassionema nitzschoides, Nitzschia longissima*, and *Pseudo-nitzschia* spp., as well as the planktonic dinoflagellate *G. catenatum* were generally associated with more saline, low-discharge, low-nitrate conditions. Of these, *D. brightwellii*, *T. nitzschoides*, *N. longissima*, and *Pseudo-nitzschia* spp. were also associated with high temperatures and upwelling. On the other hand, the abundance of the freshwater taxa *Ankistrodesmus* sp. and the tychopelagic *Navicula* spp. declined later in the growing season, with higher counts of these taxa observed in samples associated with lower temperatures, higher flows, and low salinity. This is consistent with the gradient forest cumulative density plots (Fig. 7A-E), which indicate a sharp change in cumulative importance of salinity at 13-14 PSU and of discharge at approximately 3,400 $m^3 s^{-1}$ to the abundance of the coastal diatom species, *D. brightwellii,* which increased under low discharge and high salinity. *Navicula* spp. showed an increase in cumulative importance of discharge at approximately 3,500 $m^3 s^{-1}$ and of salinity at approximately 13 PSU, with its abundance decreasing under low discharge and high salinity. *Ankistrodesmus* sp. showed a sharp change in the importance of discharge at approximately 7,079 $m^3 s^{-1}$, with its abundance decreasing when discharge declined. Temperature, upwelling, and nitrate all contributed to the abundance of c.f. *Cyclotella/Thalassiosira* spp., with increases in cell densities weakly associated with elevated temperature and upwelling index. Cumulative importance of upwelling index to the density of *N. longissima* increased at approximately 50 $m^3 s^{-1} 100 m^{-1}$, with an increase in abundance during upwelling. *T. nitzschoides* showed an increase in cumulative importance of nitrate at approximately 18 µM, with increasing abundance at lower nitrate concentrations. The gradient forest analysis indicated that the environmental variables of overall greatest importance in defining the phytoplankton assemblage in order were discharge, salinity, temperature, nitrate, and upwelling index (Fig. 7F).

Discussion

Transition to brackish-marine phytoplankton assemblage in MHW years

Every year, shifts in LCRE phytoplankton assemblages accompany the transition from riverine to marine influence in late summer (Rollwagen-Bollens et al, 2020; this study). However, oceanographic conditions accompanying MHWs – temperatures exceeding daily decadal averages by 1-2 °C and anomalously low discharge volumes - were associated with the only blooms of toxigenic species observed in the LCRE during the study period. In a study that temporally overlaps with ours, Rose et al. (2021) observed spikes in cyanobacterial biomass in late summer of 2017 and 2018 at a site 170 river km upstream of the mouth, though we only observed a muted elevation in cyanobacteria in the summer of 2017 at our downstream site. Although harmful cyanobacteria blooms do occur in parts of the Columbia River, we have not found records of HABs in the lower estuary area of interest for this study with the exception of those discussed herein. *Pseudo-nitzschia* spp. have been observed in the LCRE previously, but did not dominate the assemblage or reach bloom concentrations (Frame and Lessard 2009). Interestingly, the dominant HAB taxon differed between MHWs occurring in 2015 and 2019, with *Pseudo-nitzschia* spp. dominating the former and *G. catenatum* dominating the latter. Both of these taxa occupy marine-brackish habitats; thus, our discussion focuses on drivers of marine and brackish HABs at the LCRE site.

Our results may suggest two different potential mechanisms contributing to bloom development in the LCRE. In 2015, the estuary more closely resembled the coastal ocean in bloom composition; that is, the prolonged period of marine influence in the LCRE resulting from reduced river discharge provided sufficient habitat opportunity to allow offshore *Pseudo-nitzschia* spp. to persist at relatively high densities following tidal exchange. The importance of low discharge in creating appropriate conditions for a bloom is suggested by the timing of the bloom in the LCRE. Offshore, toxic *Pseudo-nitzschia australis* associated with the 2015 North Pacific MHW (National Centers for Coastal and Ocean Science 2015) was prevalent during the summer, while the *P.* c.f. *australis/fraudulenta* complex was not detected in the LCRE at significant concentrations until October 2015 when river flows declined below ~3,400 $m^3 s^{-1}$ and salinity was elevated (>14 PSU). More broadly, the samples collected in October of 2015 revealed higher abundances of marine phytoplankton, including *Pseudo-nitzschia* spp., at deeper depths where salinities were highest in association with the salt wedge (Kärnä and Baptista 2016). Particulate domoic acid (pDA) was detected (<100 ng L^{-1}) when *P.* c.f. *australis/fraudulenta* was present, although toxin levels were less than half the concentration that leads to accumulation in shellfish (ORHAB 2021).

In 2019, *G. catenatum* also bloomed during a period of low discharge (~ 2,800 $m^3 s^{-1}$ - 3,400 $m^3 s^{-1}$ 14-d average) with anomalously elevated temperature relative to the site decadal average. Particulate saxitoxins in water were observed during this bloom, but concentrations were lower than recreational alert levels (10 ppb or $\mu g\ L^{-1}$) for freshwater systems in Oregon, which does not currently have seawater saxitoxin health guidelines (Oregon Department of

Agriculture 2021). This bloom did not appear to have been transported into the estuary from a nearshore marine site like the 2015 *Pseudo-nitzschia* spp. bloom. Rather, it is likely to have developed *in situ* nearby the Ilwaco sampling site in Baker Bay, based on its absence in samples concurrently collected from the Columbia River South Jetty, and several other open coast sites in Oregon and Washington (data not shown, M. Rogers pers. comm., 2019). *Pseudo-nitzschia* spp. were present in very low concentrations in the LCRE during the 2019 *G. catenatum* event, but nearby coastal sites had higher abundances (data not shown), indicating a lesser degree of transport into the LCRE than observed during the 2015 bloom event. Given that many dinoflagellates including *G. catenatum* can form resistant cysts to sustain populations through long periods in marginal environments (Blackburn et al. 1989; Hallegraeff et al. 2012), it is possible that cysts transported from an unknown seed area (either offshore or within the estuary) could have seeded the bloom in the LCRE during conditions that favored its proliferation.

We identified clear shifts in phytoplankton assemblages associated with thresholds of discharge and salinity, but the mechanism by which these shifts occur is not clear from this analysis, particularly in explaining the emergence of two different HABs during the transition to marine dominance of the LCRE under low-flow conditions. The observed association of *Pseudo-nitzschia* spp. abundance in the LCRE with upwelling may be due to the effect of wind stress on the movement of the Columbia River plume, which can act as a barrier to onshore transport of marine plankton during downwelling. During upwelling winds, offshore plankton may become entrained within it or subduction may occur (Hickey et al. 2005). The *G. catenatum* bloom did not show the same association with upwelling, and occurred during a significant decreasing trend in upwelling index. Upwelling also supplies inorganic nutrients to surface coastal waters and has a proportionally greater impact on nutrient inputs to the LCRE under low flow conditions

(Bruland et al. 2008). Du et al. (2016) documented enhanced *Pseudo-nitzschia* spp. growth in coastal waters during stronger upwelling in 2015, likely due to increased nutrient availability. Nitrate in the LCRE was low in early summer of 2015 compared to other years, which is likely a result of very low discharge during this time, combined with periods of weakened upwelling. During the late summer time frame when the *Pseudo-nitzschia* spp. bloom occurred, nitrate (the preferred N source for *Pseudo-nitzschia* spp. (Cochlan et al. 2008)) increased in the LCRE during a period of stronger upwelling (Du et al. 2016). We did not collect nutrient data beyond nitrate concentrations in the LCRE for 2015-2018 so we rely on previous work in this system to interpret the impact of nutrient conditions during our study period, particularly for 2019.

In contrast, *G. catenatum* is a poor competitor for inorganic nutrients, is not likely to bloom without a source of organic nutrients, and is capable of phagotrophy (Yamamoto et al. 2004; Jeong et al. 2010)). This is consistent with our finding that *G. catenatum* was not associated with inorganic-nutrient-rich marine upwelling, despite being associated with brackish waters in the LCRE. When saline waters extend into the LCRE under low flow conditions, freshwater plankton from upriver may die from osmotic stress when they encounter salinities of 1-5 PSU (Lara-Lara 1990), and contribute to available particulate organic matter (POM) (Small et al. 1990). Long residence time during low flows may slow the flushing of these resources, particularly from lateral bays, creating an optimal food source for a phagotrophic dinoflagellate, which co-occurred with other mixotrophic plankton (e.g., *Mesodinium rubrum, Euglena* spp.). Renewing water age in the LCRE is about 20 hours during high discharge conditions, but may exceed 120 hours under low discharge and neap tide conditions in bays with weak circulation, such as our study site in Baker Bay (Kärnä and Baptista 2016). This longer flushing time observed in the late summer may retain POM and provide refuge for plankton (either transported from offshore or grown within the LCRE) that may not establish under faster flowing conditions.

Both HAB taxa observed are also well-adapted to the anomalously warm, saline habitat available in the LCRE during the MHWs that was not present under higher discharge conditions. *Pseudo-nitzschia* spp. are able to grow at temperatures up to 30 ℃ (Zhu et al. 2017). They are rarely found in low salinity waters, and exhibit high mortality rates when exposed to salinity outside 30-35 PSU (Thessen et al. 2005; Ayache et al. 2019). *G. catenatum* can grow at temperatures as high as 29 ℃, though temperate ecotypes grow optimally at temperatures between 12-18 ℃ (Hallegraeff et al. 2012), and will tolerate salinities in the range of 15-40 PSU (Blackburn et al. 1989; Band-Schmidt et al. 2004).

Our analyses suggest that declining river influence during the late summer period of two anomalously warm years (2015 and 2019) was a shared driver in creating a window of habitat availability for two different HABs. Each likely occupied this habitat through a different discharge-related mechanism – an upwelling-fed coastal bloom with tidal advection into an unusually saline LCRE and *in situ* bloom development promoted by long water renewal times and a source of POM in a brackish LCRE.

Characteristics of phytoplankton assemblage transitions

Discharge and salinity were identified as the primary predictors of phytoplankton assemblage composition in the LCRE in the gradient forest analysis. This highlights the importance of the seasonally driven environmental gradient of river dominance vs. ocean influence, and takes a further step in identifying the thresholds at which the resulting phytoplankton transition occurs. The HAB taxa observed during the study period did not exhibit large changes in the cumulative importance of environmental variables in the gradient forest analysis, possibly because they were present at undetectable or low abundance prior to the onset of the HABs. However, several assemblage shifts (e.g., declines in tychopelagic *Navicula* spp. and freshwater taxa, increasing marine pelagic taxa like *Ditylum brightwellii*) may be used to demarcate estuarine niche transitions associated with elevated risk of marine and brackish HABs to help focus monitoring efforts. It should be noted that our species composition dataset is relatively sparse compared to the continuous environmental data from the LCRE. Higher resolution plankton assemblage data may improve environmental threshold estimates of plankton niche transitions, and a larger dataset would allow validation of the gradient forest model. In addition, we only analyzed phytoplankton assemblage data for one year that did not have a MHW, and therefore cannot determine how representative the 2017 community is of typical non-MHW years. In order to better understand how MHWs influence phytoplankton assemblages, more baseline assemblage data are needed to compare anomalous events with normal variability. Although our study captures two HABs during two MHWs, the lack of historical documentation of either MHWs or marine/brackish HABs in the LCRE necessitates continued monitoring to understand the relationship between MHW and HABs in this unique habitat.

Environmental drivers of phytoplankton shifts

Our NMDS analysis with environmental vector overlay indicated that *Navicula* spp. and the freshwater *Ankistrodesmus* sp. were strongly negatively associated with salinity. Although some *Navicula* species in the LCRE are thought to be tolerant of brackish conditions (Simenstad et al. 1984), it is possible that salinity exceeded the preferred range of less salt tolerant species during the extreme low flow conditions experienced in 2015 and 2019. Changes in resuspension of tychopelagic diatoms may also influence the observed shifts in phytoplankton assemblages in our surface water samples. Mixing in the LCRE is governed by complex interactions between tidal transitions, river flow, and density gradient. During the summer low flow period, neap-spring tide transitions in stratification are less disrupted by high flow events, indicating that mixing may be more governed by tidal action. During this time, hydrodynamic models suggest the LCRE is strongly or weakly stratified for most of the tidal cycle, but experiences brief periods (1-2 days) of partial mixing during the transition between the neap-tide and the rest of the tidal month (Jay 1990). Reduced vertical mixing is one possible explanation for the observed decline in tychopelagic taxa during low flow conditions. However, studies on particle movement (Stevens et al. 2017) have focused on the main channel of the LCRE, and flow dynamics are less well understood in the LCRE lateral bays.

This analysis also showed that *Pseudo-nitzschia* spp., *T. nitzschoides*, and *N. longissima,* and *D. brightwellii* (marine pelagic taxa) were positively associated with upwelling and temperature, negatively associated with nitrate, and strongly negatively associated with discharge. *G. catenatum* and *D. brightwellii* (brackish and marine pelagic taxa) were most strongly positively associated with salinity. We observed peaks in chlorophyll in late summer of 2015 and 2019, associated with the growth of these brackish and marine taxa. In contrast, chlorophyll declined significantly throughout the study period during 2017, with very low values in late summer. This may indicate a lack of a transition to marine dominance and the associated phytoplankton assemblage that increased chlorophyll in late summer of MHW years.

As climate change is expected to alter the hydrology of the Columbia River (Hamlet and Lettenmaier 1999), the conditions observed during the described MHW years may become more common in the future. It is likely that low-snowpack, high temperature years will become more frequent, low-flow timeframes may be extended, and flows may be lower during drought conditions, creating potential for a longer, geographically larger window of ocean-influenced

LCRE. Currently this LCRE habitat is ephemeral, but has the potential to increase spatially (upriver) and temporally. Our study is limited by the number of years of LCRE phytoplankton monitoring data, making mechanistic explanation of the two different HABs observed during climatically anomalous events challenging.

Despite the increasing occurrence of algal toxin closures for Pacific Northwest beaches, most bays and estuaries remain open to shellfish harvest all year and many are not monitored for HABs to provide early warning of toxin events. Although strong freshwater flows during the winter and spring generally preclude the need for marine and brackish HAB monitoring in river-dominated west coast estuaries, we show that these HABs can develop during anomalously low summer discharge. Sustained monitoring will be essential to understand mechanisms driving estuarine HAB development in a changing climate.

References

Amaya, Dillon J., Arthur J. Miller, Shang-Ping Xie, and Yu Kosaka. 2020. Physical Drivers of the Summer 2019 North Pacific Marine Heatwave. *Nature Communications* 11 (1): 1903. https://doi.org/10.1038/s41467-020-15820-w.

Ayache, Nour, Fabienne Hervé, Véronique Martin-Jézéquel, Zouher Amzil, and Amandine M. N. Caruana. 2019. "Influence of Sudden Salinity Variation on the Physiology and Domoic Acid Production by Two Strains of Pseudo-Nitzschia Australis." *Journal of Phycology* 55 (1): 186–95. https://doi.org/10.1111/jpy.12801.

Band-Schmidt, C. J., L. Morquecho, C. H. Lechuga-Devéze, and D. M. Anderson. 2004. "Effects of Growth Medium, Temperature, Salinity and Seawater Source on the Growth of Gymnodinium Catenatum (Dinophyceae) from Bahía Concepción, Gulf of California, Mexico." *Journal of Plankton Research* 26 (12): 1459–70. https://doi.org/10.1093/plankt/fbh133.

Baptista, António M., Charles Seaton, Michael P. Wilkin, Sarah F. Riseman, Joseph A. Needoba, David Maier, Paul J. Turner, et al. 2015. "Infrastructure for Collaborative Science and Societal Applications in the Columbia River Estuary." *Frontiers of Earth Science* 9 (4): 659–82. https://doi.org/10.1007/s11707-015-0540-5.

Berdalet, Elisa, Lora E. Fleming, Richard Gowen, Keith Davidson, Philipp Hess, Lorraine C. Backer, Stephanie K. Moore, Porter Hoagland, and Henrik Enevoldsen. 2016. "Marine

Harmful Algal Blooms, Human Health and Wellbeing: Challenges and Opportunities in the 21st Century.” *Journal of the Marine Biological Association of the United Kingdom* 96 (1): 61–91. https://doi.org/10.1017/S0025315415001733.

Biela, Vr von, Ml Arimitsu, Jf Piatt, B Heflin, Jl Schoen SK Trowbridge, and Cm Clawson. 2019. Extreme Reduction in Nutritional Value of a Key Forage Fish during the Pacific Marine Heatwave of 2014-2016. *Marine Ecology Progress Series* 613 (March): 171–82. https://doi.org/10.3354/meps12891.

Blackburn, Susan I., Gustaaf M. Hallegraeff, and Christopher J. Bolch. 1989. “Vegetative Reproduction and Sexual Life Cycle of the Toxic Dinoflagellate Gymnodinium Catenatum from Tasmania, Australia.” *Journal of Phycology* 25 (3): 577–90. https://doi.org/10.1111/j.1529-8817.1989.tb00264.x.

Bond, Nicholas A., Meghan F. Cronin, Howard Freeland, and Nathan Mantua. 2015. Causes and Impacts of the 2014 Warm Anomaly in the NE Pacific. *Geophysical Research Letters* 42 (9): 3414–20. https://doi.org/10.1002/2015GL063306.

Boniface O. Fosu, S.-Y. Simon Wang, and Jin-Ho Yoon. 2016. EXPLAINING EXTREME EVENTS OF 2015 FROM A CLIMATE PERSPECTIVE. THE 2014/15 SNOWPACK DROUGHT IN WASHINGTON STATE AND ITS CLIMATE FORCING.

Brodeur, Richard D., Toby D. Auth, and Anthony Jason Phillips. 2019. Major Shifts in Pelagic Micronekton and Macrozooplankton Community Structure in an Upwelling Ecosystem Related to an Unprecedented Marine Heatwave. *Frontiers in Marine Science* 6. https://doi.org/10.3389/fmars.2019.00212.

Bruland, K. W., Lohan, M. C., Aguilar-Islas, A. M., Smith, G. J., Sohst, B., & Baptista, A. 2008. “Factors influencing the chemistry of the near-field Columbia River plume: Nitrate, silicic acid, dissolved Fe, and dissolved Mn.” *Journal of Geophysical Research: Oceans*, *113*(C2).

Cayan, Daniel R. 1996. “Interannual Climate Variability and Snowpack in the Western United States.” *Journal of Climate* 9 (5): 928–48. https://doi.org/10.1175/1520-0442(1996)009<0928:ICVASI>2.0.CO;2.

Chawla, Arun, David A. Jay, António M. Baptista, Michael Wilkin, and Charles Seaton. 2008. “Seasonal Variability and Estuary–Shelf Interactions in Circulation Dynamics of a River-Dominated Estuary.” *Estuaries and Coasts* 31 (2): 269–88. https://doi.org/10.1007/s12237-007-9022-7.

Center for Coastal Margin Observation and Prediction. 2022. “Fixed Station User Interface SATURN-03”.2021. http://www.stccmop.org/datamart/observation_network/fixedstation?id=saturn03

Clark, Martyn P., Mark C. Serreze, and Greg J. McCabe. 2001. “Historical Effects of El Nino and La Nina Events on the Seasonal Evolution of the Montane Snowpack in the Columbia and Colorado River Basins.” *Water Resources Research* 37 (3): 741–57. https://doi.org/10.1029/2000WR900305.

Clarke, K. R. 1993. Non-Parametric Multivariate Analyses of Changes in Community Structure. *Austral Ecology* 18 (1): 117–43. https://doi.org/10.1111/j.1442-9993.1993.tb00438.x.

Cloern, James E., Tara S. Schraga, and Cary Burns Lopez. 2005. Heat Wave Brings an Unprecedented Red Tide to San Francisco Bay. *Eos, Transactions American Geophysical Union* 86 (7): 66–66. https://doi.org/10.1029/2005EO070003.

Cochlan, William P., Julian Herndon, and Raphael M. Kudela. 2008. "Inorganic and Organic Nitrogen Uptake by the Toxigenic Diatom Pseudo-Nitzschia Australis (Bacillariophyceae)." *Harmful Algae*, HABs and Eutrophication, 8 (1): 111–18. https://doi.org/10.1016/j.hal.2008.08.008.

Columbia River DART, Columbia Basin Research, and University of Washington. 2021. "Pacific Ocean Coastal Upwelling Indices." 2021. http://www.cbr.washington.edu/dart/query/upwell_daily.

Costa, Pedro Reis, Maria João Botelho, and Kathi A. Lefebvre. 2010. "Characterization of Paralytic Shellfish Toxins in Seawater and Sardines (Sardina Pilchardus) during Blooms of Gymnodinium Catenatum." *Hydrobiologia* 655 (1): 89–97. https://doi.org/10.1007/s10750-010-0406-5.

Di Lorenzo, Emanuele, and Nathan Mantua. 2016. "Multi-Year Persistence of the 2014/15 North Pacific Marine Heatwave." *Nature Climate Change* 6 (11): 1042–47. https://doi.org/10.1038/nclimate3082.

Du, Xiuning, William Peterson, Jennifer Fisher, Matt Hunter, and Jay Peterson. 2016. Initiation and Development of a Toxic and Persistent Pseudo-Nitzschia Bloom off the Oregon Coast in Spring/Summer 2015. *PLOS ONE* 11 (10): e0163977. https://doi.org/10.1371/journal.pone.0163977.

Dyson, Karen, and Daniel D. Huppert. 2010. "Regional Economic Impacts of Razor Clam Beach Closures Due to Harmful Algal Blooms (HABs) on the Pacific Coast of Washington." *Harmful Algae* 9 (3): 264–71. https://doi.org/10.1016/j.hal.2009.11.003.

Ellis, Nick, Stephen J. Smith, and C. Roland Pitcher. 2012. Gradient Forests: Calculating Importance Gradients on Physical Predictors. *Ecology* 93 (1): 156–68. https://doi.org/10.1890/11-0252.1.

Federal Columbia River Power System. "The Columbia River System Inside Story." 2001. Bonneville Power Administration, U.S. Bureau of Reclamation, U.S. Army Corps of Engineers. https://www.bpa.gov/p/Generation/Hydro/hydro/columbia_river_inside_story.pdf.

Frame, E. R., & Lessard, E. J. 2009. "Does the Columbia River plume influence phytoplankton community structure along the Washington and Oregon coasts?" *Journal of Geophysical Research: Oceans*, *114*(C2).

Gao, Guang, Xin Zhao, Meijia Jiang, and Lin Gao. 2021. "Impacts of Marine Heatwaves on Algal Structure and Carbon Sequestration in Conjunction With Ocean Warming and Acidification." *Frontiers in Marine Science* 8. https://doi.org/10.3389/fmars.2021.758651.

Haertel, L., & Osterberg, C. 1967. Ecology of zooplankton, benthos and fishes in the Columbia River estuary. *Ecology*, *48*(3), 459-472.

Hallegraeff, G. M. 1993. A Review of Harmful Algal Blooms and Their Apparent Global Increase. *Phycologia* 32 (2): 79–99. https://doi.org/10.2216/i0031-8884-32-2-79.1.

Hallegraeff, Gustaaf M. 2010. Ocean Climate Change, Phytoplankton Community Responses, and Harmful Algal Blooms: A Formidable Predictive Challenge. *Journal of Phycology* 46 (2): 220–35. https://doi.org/10.1111/j.1529-8817.2010.00815.x.

Hallegraeff, G. M., S. I. Blackburn, M. A. Doblin, and C. J. S. Bolch. 2012. "Global Toxicology, Ecophysiology and Population Relationships of the Chainforming PST Dinoflagellate Gymnodinium Catenatum." *Harmful Algae*, Harmful Algae--The requirement for species-specific information, 14 (February): 130–43. https://doi.org/10.1016/j.hal.2011.10.018.

Hamlet, Alan F., and Dennis P. Lettenmaier. 1999. "Effects of Climate Change on Hydrology and Water Resources in the Columbia River Basin1." *JAWRA Journal of the American Water Resources Association* 35 (6): 1597–1623. https://doi.org/10.1111/j.1752-1688.1999.tb04240.x.

Heady, W.N., K. O'Connor, J. Kassakian, K. Doiron, C. Endris, D. Hudgens, R. P. Clark, J. and Carter, and M. G. Gleason. 2014. An Inventory and Classification of U.S. West Coast Estuaries. Arlington, VA: The Nature Conservancy. http://www.pacificfishhabitat.org/wp-content/uploads/2017/09/wc_estuaryinventory_final_report_jan15_2015.pdf.

Herfort, Lydie, Tawnya D. Peterson, Victoria Campbell, Sheedra Futrell, and Peter Zuber. 2011. "Myrionecta Rubra (Mesodinium Rubrum) Bloom Initiation in the Columbia River Estuary." *Estuarine, Coastal and Shelf Science* 95 (4): 440–46. https://doi.org/10.1016/j.ecss.2011.10.015.

Hickey, B., S. Geier, N. Kachel, and A. MacFadyen. 2005. "A Bi-Directional River Plume: The Columbia in Summer." *Continental Shelf Research* 25 (14): 1631–56. https://doi.org/10.1016/j.csr.2005.04.010.

Hobday, Alistair, Eric Oliver, Alex Sen Gupta, Jessica Benthuysen, Michael Burrows, Markus Donat, Neil Holbrook, Pippa Moore, Mads Thomsen, Thomas Wernberg, Dan Smale. 2018. "Categorizing and Naming Marine Heatwaves." *Oceanography* 31, no. 2. https://doi.org/10.5670/oceanog.2018.205.

Jay, D. A., & Smith, J. D. 1990. "Residual circulation in shallow estuaries: 1. Highly stratified, narrow estuaries." *Journal of Geophysical Research: Oceans*, *95*(C1), 711-731.

Jeong, Hae Jin, Yeong Du Yoo, Jae Seong Kim, Kyeong Ah Seong, Nam Seon Kang, and Tae Hoon Kim. 2010. "Growth, Feeding and Ecological Roles of the Mixotrophic and Heterotrophic Dinoflagellates in Marine Planktonic Food Webs." *Ocean Science Journal* 45 (2): 65–91. https://doi.org/10.1007/s12601-010-0007-2.

Kärnä, Tuomas, and António M. Baptista. 2016. Water Age in the Columbia River Estuary. *Estuarine, Coastal and Shelf Science* 183 (December): 249–59. https://doi.org/10.1016/j.ecss.2016.09.001.

Kudela, Raphael M., William P. Cochlan, Tawnya D. Peterson, and Charles G. Trick. 2006. "Impacts on Phytoplankton Biomass and Productivity in the Pacific Northwest during the

Warm Ocean Conditions of 2005." *Geophysical Research Letters* 33, no. 22. https://doi.org/10.1029/2006GL026772.

Lara-Lara, J Ruben. 1990. "Primary Production in the Columbia River Estuary I. Spatial and Temporal Variability of Properties!" *PACIFIC SCIENCE* 44: 21.

Lefebvre, K., M. Silver, S. Coale, and R. Tjeerdema. 2002. "Domoic Acid in Planktivorous Fish in Relation to Toxic Pseudo-Nitzschia Cell Densities." *Marine Biology* 140 (3): 625–31. https://doi.org/10.1007/s00227-001-0713-5.

Lefebvre, Kathi A., Brian D. Bill, Aleta Erickson, Keri A. Baugh, Lohna O'Rourke, Pedro R. Costa, Shelly Nance, and Vera L. Trainer. 2008. Characterization of Intracellular and Extracellular Saxitoxin Levels in Both Field and Cultured Alexandrium Spp. Samples from Sequim Bay, Washington. *Marine Drugs* 6 (2): 103–16. https://doi.org/10.3390/md6020103.

Lewitus, Alan J., Rita A. Horner, David A. Caron, Ernesto Garcia-Mendoza, Barbara M. Hickey, Matthew Hunter, Daniel D. Huppert, et al. 2012. Harmful Algal Blooms along the North American West Coast Region: History, Trends, Causes, and Impacts. *Harmful Algae* 19 (September): 133–59. https://doi.org/10.1016/j.hal.2012.06.009.

McCabe, Ryan M., Barbara M. Hickey, Raphael M. Kudela, Kathi A. Lefebvre, Nicolaus G. Adams, Brian D. Bill, Frances M. D. Gulland, Richard E. Thomson, William P. Cochlan, and Vera L. Trainer. 2016. "An Unprecedented Coastwide Toxic Algal Bloom Linked to Anomalous Ocean Conditions." *Geophysical Research Letters* 43 (19): 10,366-10,376. https://doi.org/10.1002/2016GL070023.

Mote, Philip W. 2006. "Climate-Driven Variability and Trends in Mountain Snowpack in Western North America." *Journal of Climate* 19 (23): 6209–20. https://doi.org/10.1175/JCLI3971.1.

National Centers for and Coastal Ocean Science. 2015. "West Coast Harmful Algal Bloom Draws Attention of Congress." 2015. https://coastalscience.noaa.gov/news/west-coast-harmful-algal-bloom-draws-attention-congress/.

Oksanen, J. 2011. Multivariate analysis of ecological communities in R: vegan tutorial. *R package version*, *1*(7), 1-43.

Oregon Department of Agriculture. 2021. "MUSSEL AND CLAM BIOTOXIN LAB RESULTS," 8.

ORHAB. (2021). *PNW hab bulletin*. UW Departments Web Server. https://depts.washington.edu/orhab/pnw-hab-bulletin/.

Piatt, John F., Julia K. Parrish, Heather M. Renner, Sarah K. Schoen, Timothy T. Jones, Mayumi L. Arimitsu, Kathy J. Kuletz, et al. 2020. Extreme Mortality and Reproductive Failure of Common Murres Resulting from the Northeast Pacific Marine Heatwave of 2014-2016. *PLOS ONE* 15 (1): e0226087. https://doi.org/10.1371/journal.pone.0226087.

Poe, Melissa R., Phillip S. Levin, Nick Tolimieri, and Karma Norman. 2015. "Subsistence Fishing in a 21st Century Capitalist Society: From Commodity to Gift." *Ecological Economics* 116 (August): 241–50. https://doi.org/10.1016/j.ecolecon.2015.05.003.

Ritzman, Jerilyn, Amy Brodbeck, Sara Brostrom, Scott McGrew, Stacia Dreyer, Terrie Klinger, and Stephanie K. Moore. 2018. "Economic and Sociocultural Impacts of Fisheries Closures in Two Fishing-Dependent Communities Following the Massive 2015 U.S. West Coast Harmful Algal Bloom." *Harmful Algae* 80 (December): 35–45. https://doi.org/10.1016/j.hal.2018.09.002.

Roberts, Shane D., Paul D. Van Ruth, Clinton Wilkinson, Stella S. Bastianello, and Matthew S. Bansemer. 2019. "Marine Heatwave, Harmful Algae Blooms and an Extensive Fish Kill Event During 2013 in South Australia." *Frontiers in Marine Science* 6. https://doi.org/10.3389/fmars.2019.00610.

Rogers-Bennett, L., and C. A. Catton. 2019. Marine Heat Wave and Multiple Stressors Tip Bull Kelp Forest to Sea Urchin Barrens. *Scientific Reports* 9 (1): 15050. https://doi.org/10.1038/s41598-019-51114-y.

Rollwagen-Bollens, Gretchen, Stephen Bollens, Eric Dexter, and Jeffery Cordell. 2020. "Biotic vs. Abiotic Forcing on Plankton Assemblages Varies with Season and Size Class in a Large Temperate Estuary." *Journal of Plankton Research* 42 (2): 221–37. https://doi.org/10.1093/plankt/fbaa010.

Rose, V, G Rollwagen-Bollens, Sm Bollens, and J Zimmerman. 2021. "Seasonal and Interannual Variation in Lower Columbia River Phytoplankton (2005-2018): Environmental Variability and a Decline in Large Bloom-Forming Diatoms." *Aquatic Microbial Ecology* 87: 29–46. https://doi.org/10.3354/ame01967.

Simenstad, Charles, Lawrence Small, and David McIntire. 1990. "Consumption Processes and Food Web Structure in the Columbia River Estuary." *Progress in Oceanography* 25 (1–4): 271–97. https://doi.org/10.1016/0079-6611(90)90010-Y.

Simenstad, Charles A, David A Jay, C. David McIntire, Willa Nehlson, Christopher R Sherwood, and Lawrence Small. 1984. "The Dynamics of the Columbia River Estuarine Ecosystem Volume II." Columbia River Estuary Data Development Program

Simpson, E. H. 1949. "Measurement of Diversity." *Nature* 163 (4148): 688–688. https://doi.org/10.1038/163688a0.

Simpson, Gavin L. 2018. "Modelling Palaeoecological Time Series Using Generalized Additive Models." https://doi.org/10.1101/322248.

Small, Lawrence F., C. David McIntire, Keith B. MacDonald, J. Ruben Lara-Lara, Bruce E. Frey, Michael C. Amspoker, and Ted Winfield. 1990. "Primary Production, Plant and Detrital Biomass, and Particle Transport in the Columbia River Estuary." *Progress in Oceanography* 25 (1): 175–210. https://doi.org/10.1016/0079-6611(90)90007-O.

Stevens, A.W., Gelfenbaum, G., MacMahan, J., Reniers, A.J.H.M., Elias, E.P., Sherwood, C.R., Carlson, E.M. 2017. "Oceanographic measurements and hydrodynamic modeling of the mouth of the Columbia River, Oregon and Washington", 2013: U.S. Geological Survey data release, http://dx.doi.org/10.5066/F7NG4NS1.

Tassone, Spencer J., Alice F. Besterman, Cal D. Buelo, Jonathan A. Walter, and Michael L. Pace. 2022. "Co-Occurrence of Aquatic Heatwaves with Atmospheric Heatwaves, Low Dissolved Oxygen, and Low PH Events in Estuarine Ecosystems." *Estuaries and Coasts* 45 (3): 707–20. https://doi.org/10.1007/s12237-021-01009-x.

Thessen, Anne E., Quay Dortch, Michael L. Parsons, and Wendy Morrison. 2005. “Effect of Salinity on Pseudo-Nitzschia Species (Bacillariophyceae) Growth and Distribution.” *Journal of Phycology* 41 (1): 21–29. https://doi.org/10.1111/j.1529-8817.2005.04077.x.

Tohver, Ingrid M., Alan F. Hamlet, and Se-Yeun Lee. 2014. Impacts of 21st-Century Climate Change on Hydrologic Extremes in the Pacific Northwest Region of North America. *JAWRA Journal of the American Water Resources Association* 50 (6): 1461–76. https://doi.org/10.1111/jawr.12199.

Trainer, Vera L., Marc Suddleson. 2005. “Monitoring Approaches for Early Warning of Domoic Acid Events in Washington State.” *Oceanography* 18 (2): 228-237. https://doi.org/10.5670/oceanog.2005.56.

Van Dolah F M. 2000. Marine Algal Toxins: Origins, Health Effects, and Their Increased Occurrence. *Environmental Health Perspectives* 108 (suppl 1): 133–41. https://doi.org/10.1289/ehp.00108s1133.

United States Geological Survey, National Streamflow Information Program. 2022. “USGS 14246900 COLUMBIA RIVER AT PORT WESTWARD, NEAR QUINCY, OR.” 2021. https://waterdata.usgs.gov/nwis/uv?site_no=14246900

Wetz, Michael S., and David W. Yoskowitz. 2013. An ‘Extreme’ Future for Estuaries? Effects of Extreme Climatic Events on Estuarine Water Quality and Ecology. *Marine Pollution Bulletin* 69 (1): 7–18. https://doi.org/10.1016/j.marpolbul.2013.01.020.

Wood, Simon N. 2017. *Generalized Additive Models: An Introduction with R*. Second edition. Chapman & Hall/CRC Texts in Statistical Science. Boca Raton: CRC Press/Taylor & Francis Group.

Yamamoto, T., Oh, S. J., & Kataoka, Y. 2004. “Growth and uptake kinetics for nitrate, ammonium and phosphate by the toxic dinoflagellate Gymnodinium catenatum isolated from Hiroshima Bay, Japan.” *Fisheries Science*, *70*(1), 108-115.

Zhu, Zhi, Pingping Qu, Feixue Fu, Nancy Tennenbaum, Avery O. Tatters, and David A. Hutchins. 2017. “Understanding the Blob Bloom: Warming Increases Toxicity and Abundance of the Harmful Bloom Diatom Pseudo-Nitzschia in California Coastal Waters.” *Harmful Algae* 67 (July): 36–43. https://doi.org/10.1016/j.hal.2017.06.004.

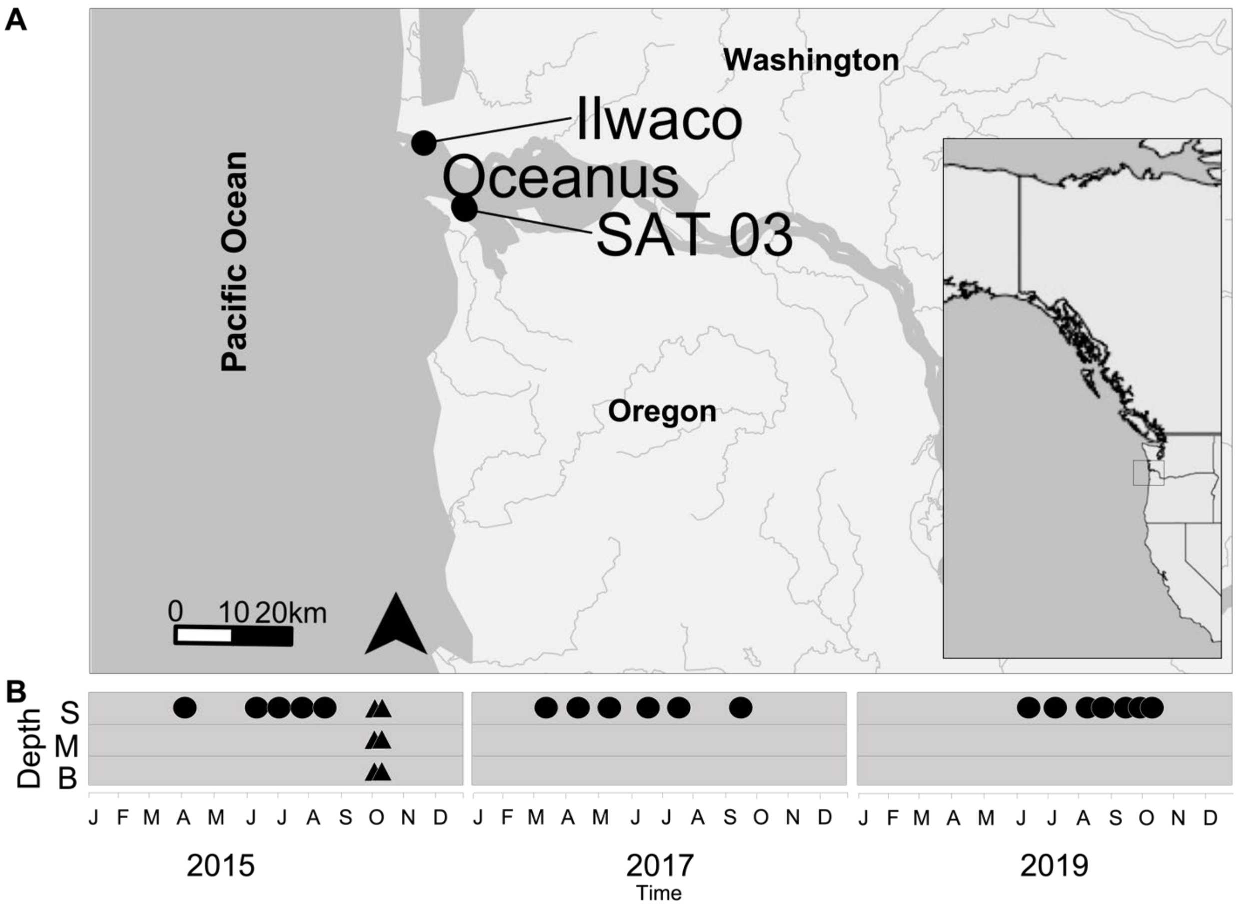

Fig. 1 Map of Lower Columbia River Estuary with regional inset (A) and phytoplankton sampling scheme (B). (A) The Columbia River forms part of the Oregon-Washington border. Phytoplankton and nutrient samples were collected from Ilwaco and Oceanus sites. Environmental data were collected from sensors at Saturn 03 site. Discharge data were collected upstream of the close-up map, and upwelling index was reported for Lincoln City (Oregon Coast). (B) Each point on the timeline represents a phytoplankton sampling event, with the depth of the sample specified on the y-axis (S = surface, M= mid-water column, B = bottom). Circles represent sampling from the Ilwaco site and triangles represent sampling from the R/V Oceanus. Our sampling scheme combined long-term, low frequency, surface samples with short-term, high-frequency, samples of the whole water column. This allowed for characterization of phytoplankton assemblages at multiple temporal and spatial scales.

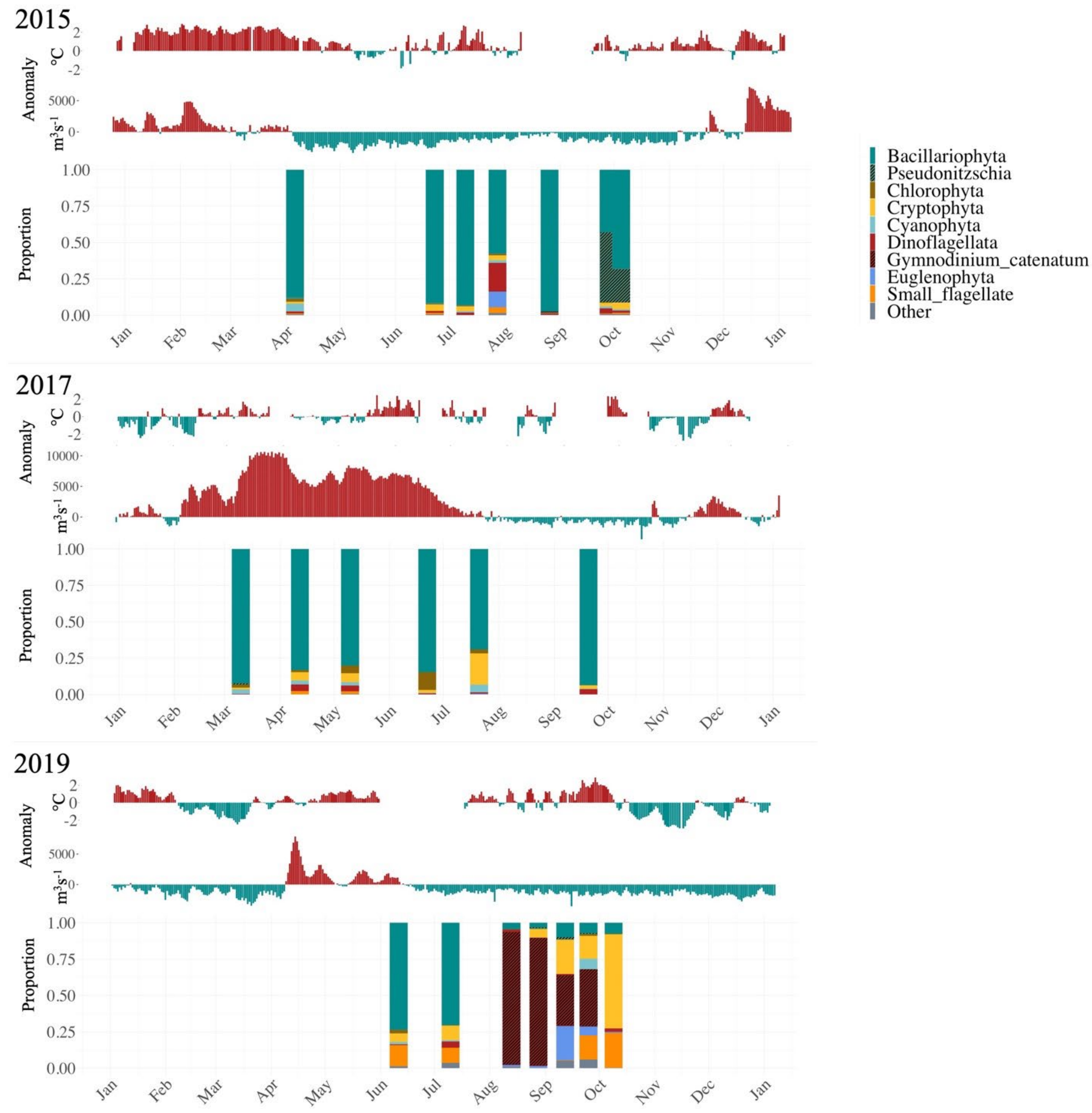

Fig. 2 Bar plots of phytoplankton assemblage composition (bottom) with temperature anomaly in degrees Celsius (top) for 2015, 2017, and 2019. Phytoplankton taxa are divided into phyla (Bacillariophyta Chlorophyta, Cryptophyta, Cyanophyta, Dinoflagellata, Euglenophyta) and agglomerative groups (Small flagellates and Other, which includes a combination of other phyla that were relatively rare). All phytoplankton samples were taken at the surface, except for the October 2015 samples, which are shown as an average of phytoplankton samples from the surface, middle and bottom of the water column. The harmful algal blooms observed during the study period

(*Pseudo-nitzschia* spp. and *Gymnodinium catenatum*) are given their own group and color (striped). Temperature anomaly (difference from decadal daily average at Saturn-03 site) is shown on the same time-scale as phytoplankton bar plots, with warmer-than-average days shown in red, cooler-than-average days shown in blue, and gaps in the time series indicating missing values.

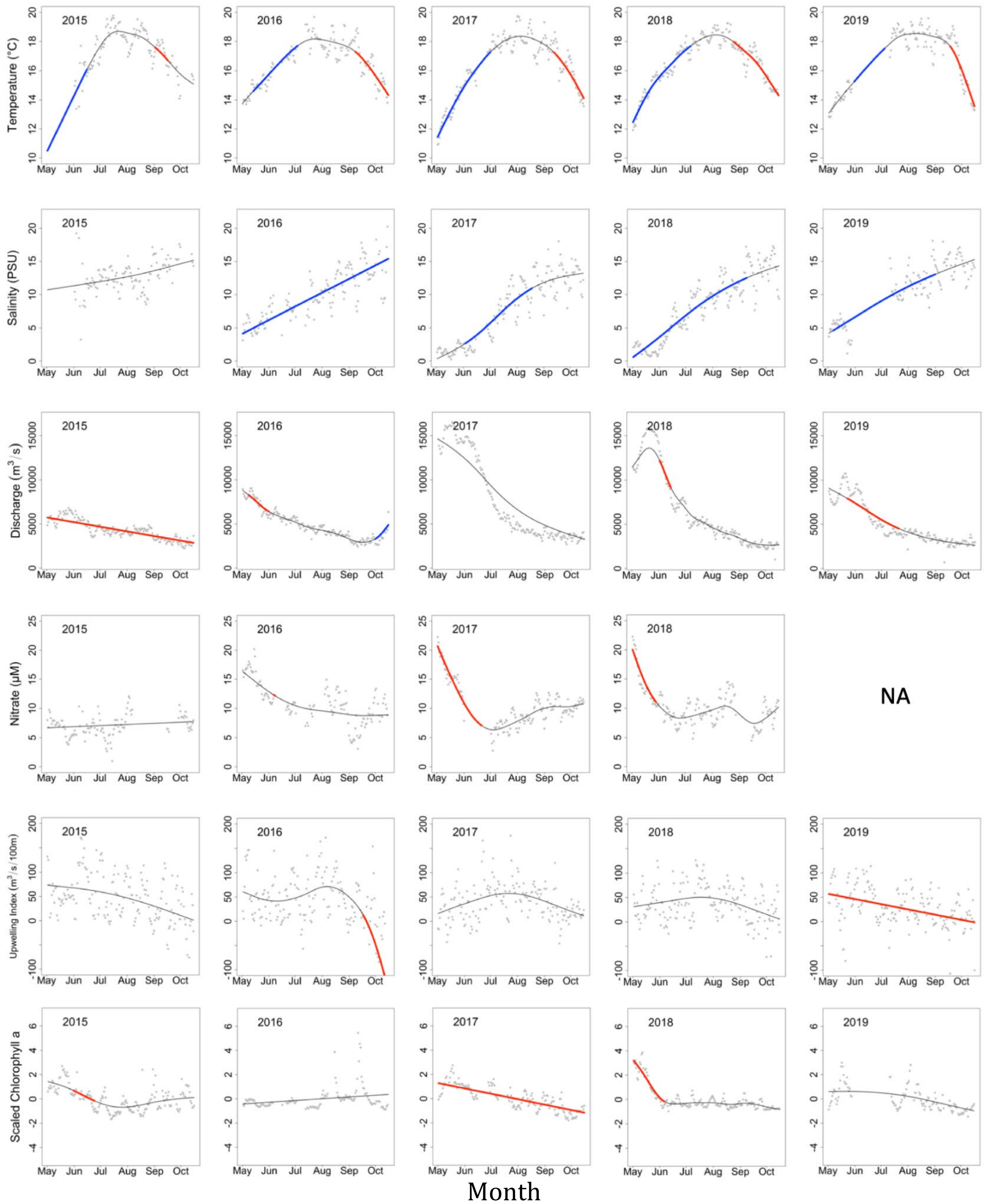

Fig. 3 GAMMs provide a characterization of environmental conditions during the growing season (May-October) of each year from 2015 - 2019, with significantly increasing modeled time frames displayed in blue, and significantly

decreasing periods shown in red. Chlorophyll a values for each year were scaled (z-scores) to account for inter-annual differences in sensor calibration. NA: Nitrate data in 2019 was missing.

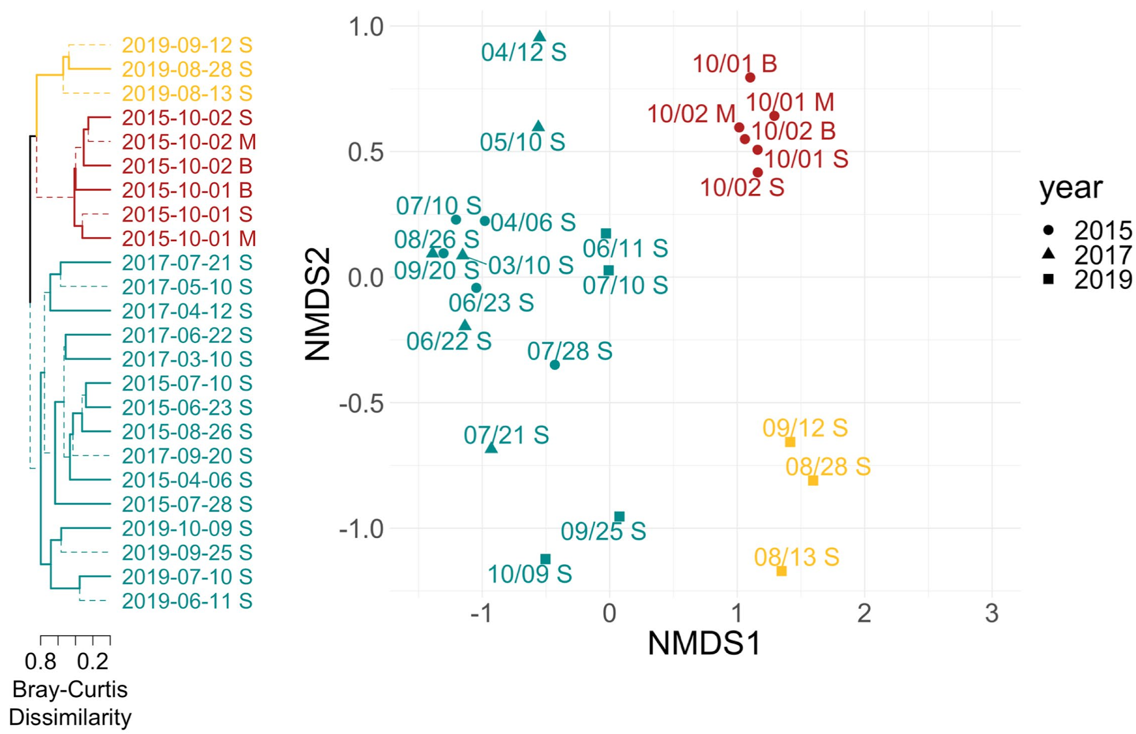

Fig. 4 Two-dimensional ordination using non-metric multidimensional scaling (NMDS) of phytoplankton assemblage data with hierarchical clustering analysis. Each point represents a phytoplankton sampling date and depth (S = surface, M = mid-water column, B = bottom), with more similar communities placed closer to each other. Stress value for the NMDS is 0.12. Shapes depict sampling year (circle = 2015, triangle = 2017, square = 2019). Colors depict cluster identity and dashed lines indicate branches leading to distinct sub-trees.

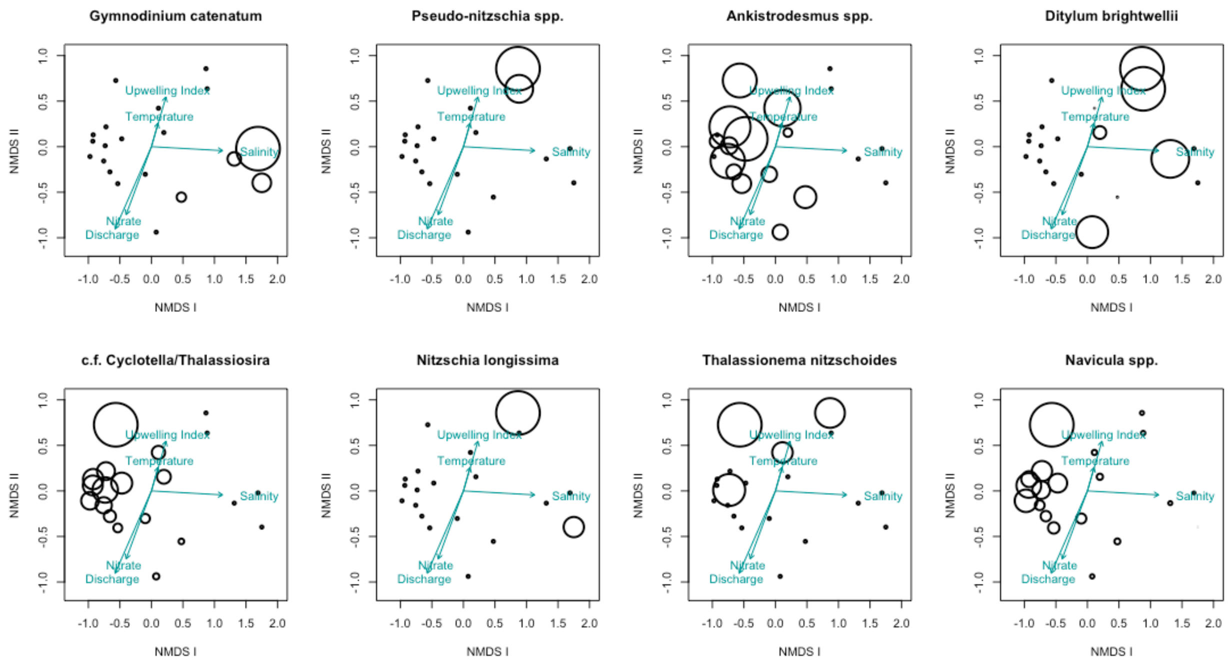

Fig. 5 Non-metric multidimensional scaling plots of phytoplankton assemblage from Ilwaco Harbor samples from 2015, 2017, and 2019, with bubble size proportional to the relative abundance of the selected taxa. Environmental vectors that correspond to the important physical drivers in the gradient forest analysis are overlaid. Phytoplankton taxa were selected either for toxin-production potential (*Pseudo-nitzschia spp.* and *Gymnodinium catenatum*) or because of a notable shift in cumulative importance over the gradient range of environmental predictors in the gradient forest analysis. Where multiple samples were taken (i.e. at different depths) on the same day, phytoplankton abundances were averaged. All measurements of environmental variables corresponding to phytoplankton sampling dates are 14-day moving averages leading up to the date of phytoplankton sampling. Units corresponding to the environmental vectors are: discharge (m^3s^{-1}), temperature (°C), salinity (PSU), nitrate (µM), upwelling index (m^3 s^{-1} 100m offshore transport).

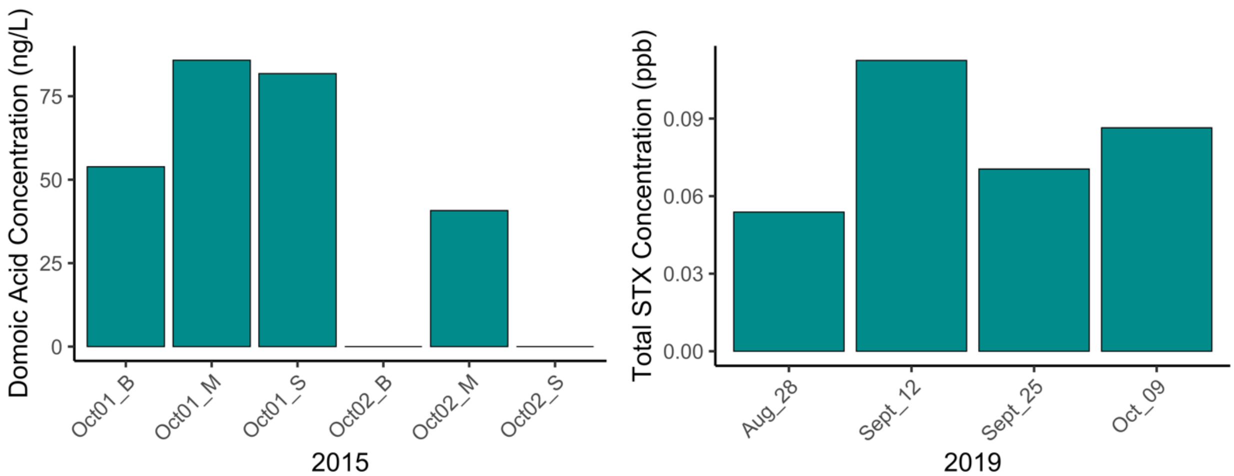

Fig. 6 Concentrations of particulate algal toxins, domoic acid (ng/L) and total saxitoxins (ppb). Domoic acid samples were taken aboard the R/V Oceanus on October 1st and 2nd of 2015 during a bloom of *Pseudo-nitzschia* spp. and total saxitoxin samples were collected from Ilwaco Harbor in August-October of 2019. For each date and depth n=1.

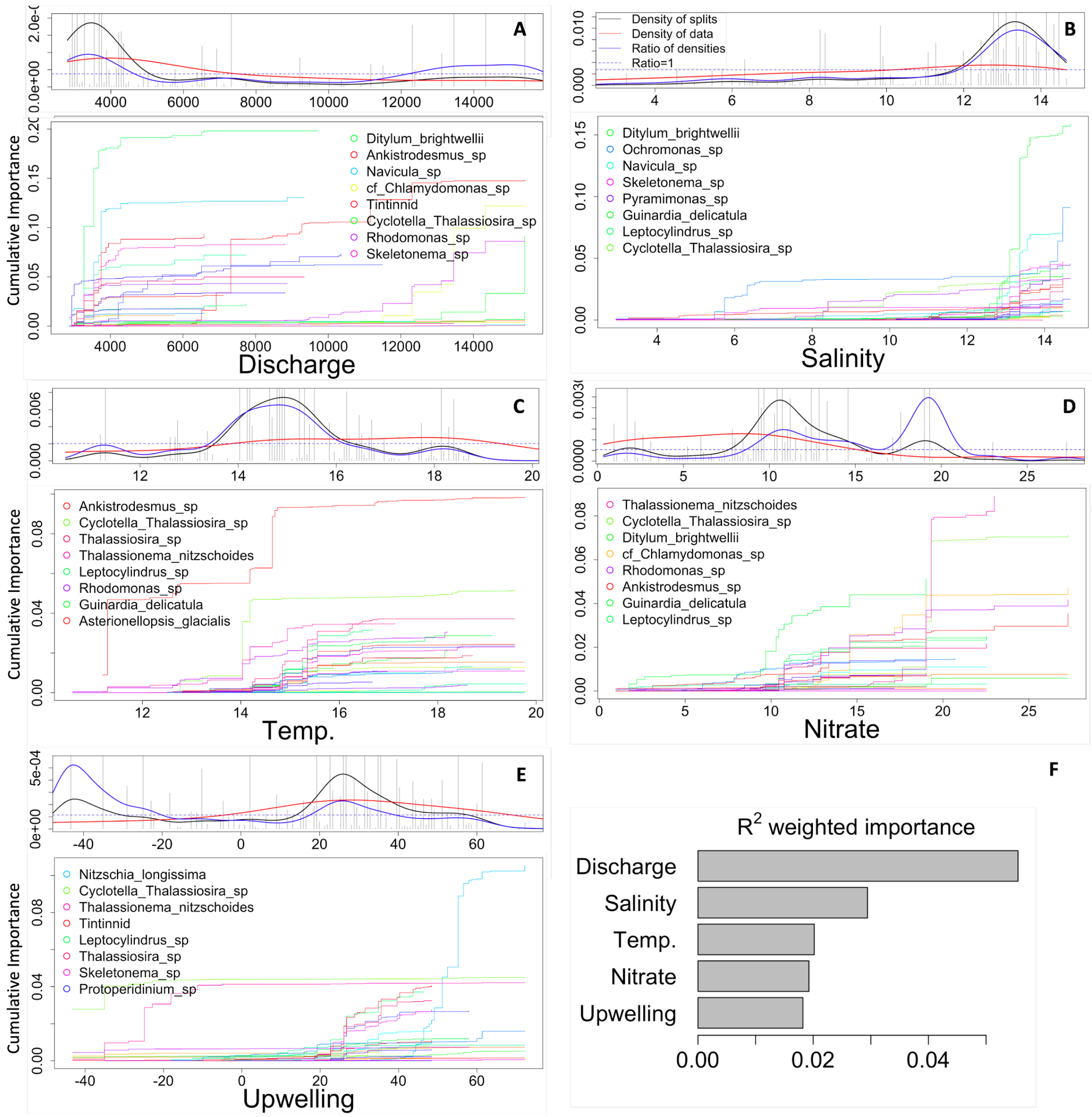

Fig. 7 Gradient forest analysis shown as split density (top, A-E) and cumulative density (bottom, A-E) plots, and overall weighted importance of each predictor (F). (Top panel, A-E) Y axis shows density, x axis shows scale of corresponding predictor variable. Black line shows density of splits from regression trees, red line and gray bars show density of data. Blue line shows the ratio of split density to data density – above dotted blue line indicates that split density is higher than data density. (Bottom panel, A-E) Y axis shows cumulative importance of each variable to the abundance of several phytoplankton taxa ((A) Discharge ($m^3 s^{-1}$), (B) Salinity (PSU), (C) Temperature (°C), (D) Nitrate (µM), (E) Upwelling Index (m^3 s^{-1} 100m offshore transport) to a given species. Different taxa are designated by different colored lines. (F) Overall importance, R^2 for each predictor of the physical drivers.

Number of day equivalents of Salinity Exceeding 15, 25, 30 PSU (d)					
	2015	2016	2017	2018	2019
>15 PSU					
2.4m	59.83	53.96	45.50	60.00	72.46
8.2m	18.29	5.00	11.04	10.79	12.75
13.0m	156.75	186.88	174.33	215.25	162.67
>25 PSU					
2.4m	7.13	3.75	4.38	3.88	3.88
8.2m	17.38	29.21	36.04	42.13	29.33
13.0m	18.04	47.46	51.13	64.75	55.42
>30 PSU					
2.4m	0.33	0.00	0.13	0.04	0.21
8.2m	1.88	0.54	4.96	2.79	0.54
13.0m	2.42	1.88	15.38	14.71	4.88

Hourly averages of salinity used to calculate number of day equivalents during June-September.

Table 1 Day equivalents of salinity exceeding 15, 25, and 30 PSU during summer season (June 1st - September 30th) at the Saturn 03 station. Salinity measured at 2.4 m, 8.2 m, and 13.0 m depth. Hourly averages used to calculate day equivalents, with missing hourly salinity measurements imputed using seasonal decomposition-based imputation.

Number of day equivalents of Temperature Exceeding 15, 18, 20 °C (d)					
	2015	2016	2017	2018	2019
>15 °C					
2.4m	89.04	76.63	92.08	106.25	73.46
8.2m	24.46	45.54	43.29	55.08	68.04
13.0m	15.75	39.75	19.13	35.50	49.63
>18 °C					
2.4m	48.96	38.29	46.25	45.88	47.38
8.2m	3.21	8.13	7.54	8.96	14.08
13.0m	2.50	4.58	2.25	3.88	6.00
>20 °C					
2.4m	18.29	5.00	11.04	10.79	12.75
8.2m	0.54	0.04	0.04	1.08	1.00
13.0m	0.25	0.63	0.25	0.75	0.25

Hourly averages of temperature used to calculate number of day equivalents during June-September.

Table 2 Day equivalents of temperature exceeding 15, 18, and 20 °C during summer season (June 1st - September 30th) at the Saturn 03 Station. Temperature measured at 2.4 m, 8.2 m, and 13.0 m depth. Hourly averages used to calculate day equivalents, with missing hourly temperature measurements imputed using seasonal decomposition-based imputation.

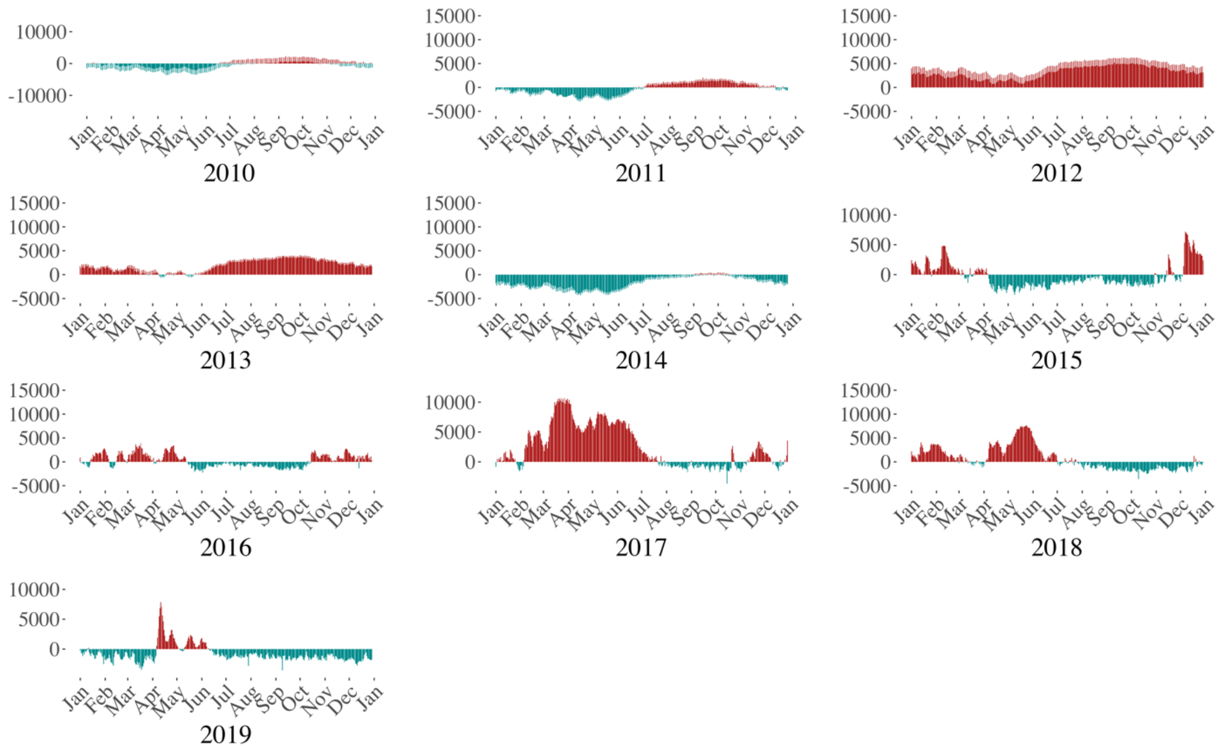

S1 Daily discharge anomaly for 2010 – 2019 compared to daily decadal average. Discharge data from USGS Quincy Station. Red bars indicate a positive discharge anomaly, blue bars indicate a negative anomaly.